Effects of the sludge physical-chemical properties on its microwave drying performance

Kocbek, Eva; Garcia, Hector A.; Hooijmans, Christine M.; Mijatović, Ivan; Kržišnik, Davor; Humar, Miha; Brdjanovic, Damir

DOI
10.1016/j.scitotenv.2022.154142

Publication date
2022

Document Version
Final published version

Published in
Science of the Total Environment

Science of the Total Environment 828 (2022) 154142

Contents lists available at ScienceDirect

Science of the Total Environment

journal homepage: www.elsevier.com/locate/scitotenv

Effects of the sludge physical-chemical properties on its microwave drying performance

Eva Kocbek [a,b,c,*], Hector A. Garcia [b], Christine M. Hooijmans [b], Ivan Mijatović [c], Davor Kržišnik [d], Miha Humar [d], Damir Brdjanovic [a,b]

[a] Department of Biotechnology, Delft University of Technology, Van der Maasweg 9, 2629 HZ Delft, the Netherlands
[b] Department of Water Supply, Sanitation and Environmental Engineering, IHE-Delft Institute for Water Education, Westvest 7, 2611 AX Delft, the Netherlands
[c] Tehnobiro d.o.o., Heroja Nandeta 37, 2000 Maribor, Slovenia
[d] Department of Wood Science and Technology, Biotechnical Faculty, University of Ljubljana Jamnikarjeva 101, SI-1000 Ljubljana, Slovenia

HIGHLIGHTS

- The quantity and distribution of water molecules in sludge affect the microwave drying performance.
- The distribution of free and bound water is affected by sludge hydrophobicity.
- Sludge with a higher fat and oil content has a higher energetic value and hydrophobicity.
- The material's ability to absorb microwave energy influences the electrical demand and throughput of the microwave system.

GRAPHICAL ABSTRACT

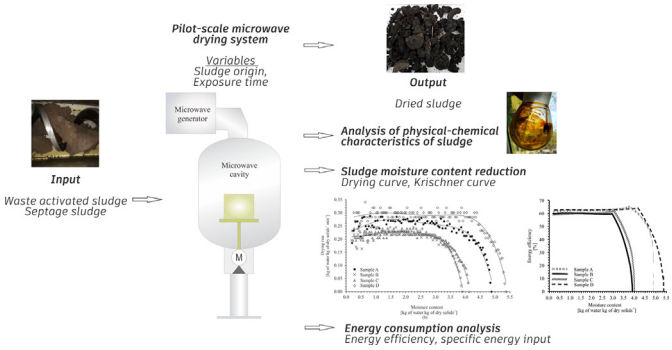

ARTICLE INFO

Article history:
Received 5 October 2021
Received in revised form 31 January 2022
Accepted 21 February 2022
Available online 25 February 2022

Editor: Yifeng Zhang

Keywords:
Microwave irradiation
Sludge drying
Energy efficiency

ABSTRACT

Thermal drying is an effective sludge treatment method for dealing with large volumes of sludge. Microwave (MW) technology has been proposed as an effective and efficient technology for sludge drying. The physical-chemical properties of the sludge depend both on the origin of the sludge, as well as on the treatment process at which the sludge has been exposed. The physical-chemical properties of the sludge affect the performance and the subsequent valorisation and management of the sludge. This study evaluated the effect of certain physical-chemical properties of the sludge (moisture content, organic content, calorific value, porosity, hydrophobicity, and water-sludge molecular interaction, among others) on the MW sludge drying and energy performance. Four different types of sludge were evaluated collected from municipal wastewater treatment plants and septic tanks. The performance of the MW system was assessed by evaluating the sludge drying rates, exposure times, energy efficiencies and power input consumed by the MW system and linking the MW drying performance to the sludge physical-chemical properties. The results confirmed that MW drying substantially extends the constant drying period associated with unbound water evaporation, irrespective

Abbreviations: C-WAS, centrifuged waste activated sludge; Cu, copper; c_p, specific heat capacity [J kg^{-1} $°C^{-1}$]; Cr, chromium; D_R, drying rate [kg of water kg of dry $solids^{-1}$ min^{-1}]; DS, dry solids [%]; DVS, dynamic vapour sorption; E, electric field intensity [V m^{-1}]; EMC, equilibrium moisture content [kg of water kg of dry $solids^{-1}$]; f, frequency [Hz]; H, hydrogen; HEM, N-hexane-extractable materials; H^{st}, total isosteric heat of sorption [kJ kg^{-1}]; h_{st}, net heat of sorption [kJ kg^{-1}]; H_v, latent heat of evaporation of pure water [kJ kg^{-1}]; m_d, total mass of dry solids in the sample; m_{eva}, amount of evaporated moisture (water) [kg]; m_{sample}, initial sample mass [kg]; m_t, sample mass [kg] at time t; MW, microwave; Ni, nickel; p, vapour partial pressure [kPa]; Pb, lead; P_d, amount of absorbed power per unit volume [W m^{-3}]; $P_{in;elect}$, input power [kW]; $P_{out;micr}$, output power [kW]; PP, polypropylene; R, universal gas constant [kJ kg^{-1} $°C^{-1}$]; RH, relative humidity [%]; S, sulphur; SS, septage sludge; SEI, specific energy input [kJ kg^{-1} of sludge]; S_{11}, the reflection coefficient [−]; t, exposure time [min]; T, temperature [°C]; TC, total carbon; TN, total nitrogen; TS, total solids; tanδ, loss tangent coefficient; VS, volatile solids; WWTP, wastewater treatment plant; Zn, zinc; β, heating rate [°C s^{-1}]; X, sludge moisture content [kg of water kg of dry $solids^{-1}$]; ε″, dielectric loss factor [−]; ε′, dielectric constant [−]; $ε_0$, permittivity of free space [8.85 × 10^{-12} fm^{-1}]; ρ, density [kg m^{-3}]; $μ_{en}$, energy efficiency [%].

* Corresponding author at: Department of Biotechnology, Delft University of Technology, Van der Maasweg 9, 2629 HZ Delft, the Netherlands.
E-mail address: info@tehnobiro.eu (E. Kocbek).

http://dx.doi.org/10.1016/j.scitotenv.2022.154142

Water sorption properties
Latent heat requirement

of the sludge sample evaluated. However, the duration and intensity were determined to depend on the dielectric properties of the sludge, particularly on the distribution of bound and free water. Sludge samples with a higher amount of free and loosely bound water absorbed and converted MW energy into heat more efficiently than sludge samples with a lower amount of free water. As a result, the sludge drying rates increased and the constant drying rate period prolonged; hence, leading to an increase in MW drying energy efficiency. The availability of free and loosely bound water molecules was favoured when hydrophobic compounds, e.g., oils and fats, were present in the sludge.

1. Introduction

On-site sanitation facilities and municipal wastewater treatment plants (WWTPs) generate significant amounts of sludge which needs to be treated before its final disposal or reuse (Kelessidis and Stasinakis, 2012). The sludge, if not correctly managed, can eventually harm the natural resources and affect the public health. However, if properly treated several valuable resources can be recovered (Kehrein et al., 2020). The sludge contains large amounts of organic matter, nitrogen, and phosphorus. Nonetheless, the sludge may also contain pathogens and contaminants such as heavy metals and organic substances which may limit its reuse as a fertilizer. Particularly, municipal sludge receiving contributions from industries and hospitals may exhibit some of these issues (Kroiss and Zessner, 2007). Therefore, both the sludge characteristics, as well as the sludge management strategies determine the subsequent reuse or disposal possibilities of the sludge and the potential environmental and/or public health impacts (Đurđević et al., 2020). Typically strategies commonly used to manage/treat the sludge include (co-) incineration, (co-) composting, and agricultural amendment, among others (Gomes et al., 2019). In all cases, there are both significant energy expenditures, as well as management issues due to the elevated water content of the sewage sludge with sludge moisture contents as high as approximately 98%. Typically, sludge moisture contents for treated sewage sludge of 60% and 15% should be reached for agricultural reuse and for energy recovery applications such as (co-) incinerations, respectively (Kamran and Gao, 2020; Lam et al., 2020). The high moisture content of the raw sludge also influences its collection (due to the large sludge volumes requiring collection), the transportation costs, and the frequency at which the sludge needs to be collected, among others. Thus, the high moisture content of the raw sludge impact on both the provision of proper sludge management strategies, as well as on the related treatment costs. In recent years, mechanical and thermal dewatering methods have been proposed as suitable alternatives for sludge treatment to be applied at the WWTP (Flaga, 2005). Mechanical dewatering can reduce the sludge moisture content up to approximately 70% and thermal drying up to approximately 5%. Currently available thermal dewatering/drying systems include belt dryers, rotary dryers, drum dryers, paddle, disc dryers, solar air heaters, and the recently introduced microwave (MW) dryer systems. (Ohm et al., 2009; Mujumdar, 2014; Khanlari et al., 2020).

Microwave irradiation has been presented as a viable technology for sludge drying achieving sludge volume reductions higher than 90% and reduce/eliminate the pathogen content present in the sludge including *E. coli*, *Ascaris lumbricoides eggs*, *Staphylococcus aureus*, and *Enterococcus faecalis* at much shorter exposure times compared to traditional drying methods such as hot air-drying techniques (Dominguez et al., 2004; Hong et al., 2004, 2006; Pino-Jelcic et al., 2006; Mawioo et al., 2016a, 2016b, 2017; Kocbek et al., 2020; Guo et al., 2021). MWs are electromagnetic waves in the range between 37.24 and 12.24 cm (i.e., frequencies of 915 and 2450 MHz, respectively) (Haque, 1999; Bilecka and Niederberger, 2010). The primary mechanism by which nonionizing electromagnetic energy is converted into heat during MW treatment is attributed to the dipolar polarisation of certain compounds in the irradiated material (Stuerga, 2006). The electric field applies a torque that serves to induce a rotational motion of all the molecules with a permanent dipole moment such as the water molecules present in the sludge (Stuerga, 2006). The oscillating electromagnetic field generates a series of changes that are resisted by the water molecules. This results in frictional, elastic, inertial, and molecular forces that increase the overall temperature of the irradiated material (Mishra and Sharma, 2016). In such way, the electromagnetic energy is converted into heat. The alternating electric field energy positioned outside of the absorbing material is irreversibly absorbed, resulting in a quick "volumetric" heating with an inverted temperature profile; i.e., upon exposure to MW radiation, the MW penetrate the material which generates heat leading to a quick sanitation and sludge mass/volume reduction. The volumetric heating effect has been reported to substantially enhance the system throughput capacity in sludge treatment systems leading to rapid reductions in the sludge volume and mass, while simultaneously mitigating the chances of disease outbreaks related to excreta health threats through pathogen inactivation (Mawioo et al., 2016a, 2016b, 2017; Kocbek et al., 2020). Advantages of MW drying applications also include fast process start-up and shutdown, lower adverse effects on global warming, if renewable energy sources can produce the electrical energy needs for the MW, and low footprint needs (Maskan, 2000, 2001; Kouchakzadeh and Shafeei, 2010; Kocbek et al., 2021). The system's high throughput capacity enable the system to be containerized (manufactured in a single container) and mounted on a trailer to perform in-situ sludge treatment (Kocbek et al., 2021). Therefore, possibly alleviating issues related to the management of faecal sludge (collection, transport and treatment) which have been reported to be inadequate, and in some cases to be completely absent in both urban and rural areas (Peal et al., 2014).

The heat transfer process is regulated by the dielectric loss tangent (tan δ) of the irradiated material defined as the ratio between the dielectric loss factor (ε″) and the dielectric constant (ε′). The dielectric loss factor represents the conversion of the electromagnetic energy into heat, while the dielectric constant depicts the ability of the material to store electromagnetic energy. Therefore, a material characterized by a high dielectric loss factors and a low dielectric constant (i.e., a high tan δ), such as the sludge, can be efficiently heated by applying MW radiation (Antunes et al., 2018). The tan δ of the irradiated material is a relevant factor when applying MW energy, and this property may change among the various MW irradiated materials. Particularly, the tan δ may significantly change depending on the physical-chemical characteristics of the sludge such as the sludge moisture and organic content. In fact, Mawioo et al. (2017) irradiated municipal sludge, septage sludge (SS), and fresh faecal sludge aiming at sludge sterilization and drying. The authors reported complete bacterial inactivation and sludge drying up to a final moisture content of 5%. Moreover, the authors reported a strong dependence of the MW performance on the physical-chemical characteristics of the sludge. For instance, the fresh faecal sludge samples, exhibiting the lowest initial moisture content of all the evaluated sludge samples of 77%, were dried much faster and demanding less energy compared to the other evaluated types of sludge. Therefore, the initial moisture content seemed to be one of the key physical-chemical sludge properties when MW drying the sludge. However, the authors also reported faster temperature increments and faster water evaporation rates when irradiating waste activated sludge (WAS) compared to when irradiating SS. The moisture content of the WAS was much higher than the moisture content of the SS; then, showing opposite trends as previously described. The authors suggested that the disparities concerning the drying rates and exposure times could be attributed not only to the moisture content, but also to the organic matter content, which was higher in WAS (75%) than in SS (55%). Mawioo et al. (2017) hypothesized that the organic compounds present in the sludge such as carbohydrates and proteins could exhibit high dielectric loss tangent factors, leading to an increase on the amount of MW energy converted into heat. However, the organic matter (mostly

carbohydrates and proteins) has also been reported to exhibit a negative impact on the MW drying performance (Dealler et al., 1992; Léonard et al., 2004). The organic matrix present in the sludge is composed of organic compounds which some of them may exhibit hydrophilic and polar groups increasing the chances of water molecules to strongly bind to such groups. Thus, such a strong bonding between the water molecules and the organic components in the sludge counteract the effects caused by the MW radiation related to promoting the rotation of the free (not bound) water molecules (Jones and Or, 2003; Pickles et al., 2014). A fraction of the water molecules present in the organic matrix in the sludge would exist in a relatively free liquid form; however, some of the water molecules would be attached to the organic matrix of the sludge tightly bound to the sludge (Vesilind, 1994). Thus, such strong binding would hinder the rotation of the water molecules negatively impacting the conversion of the electromagnetic energy into heat; so, making the MW drying process less efficient (Jones and Or, 2003; Pickles et al., 2014). As such, knowing precisely the physical-chemical properties of the sludge such as the water content and the organic content (among others) would contribute to better predict the MW drying performance of different types of sludge.

The physical-chemical characteristics of the sludge are determined by both the origin of the sludge, and by the treatment processes at which the sludge has gone through. Such characteristics of the sludge strongly influence on subsequent sludge drying processes such as the MW sludge drying. Particularly, the physical-chemical properties will determine the efficacy of the MW treatment for the sanitization and drying of the different types of sludge, as well as the energy expenditures involved in such processes. The effects of the sludge properties on the MW drying performance have not been thoroughly reported in the literature; therefore, they need to be assessed. This research addressed such needs directly. This research aims firstly at determining the physical-chemical properties of different types of sludge originated from different municipal WWTPs and on-site facilities; such sludge properties were also related to the origin of the sludge and to the wastewater treatment processes at which the sludge was exposed. The sludge physical-chemical properties determined in this study included: moisture content, organic content, elemental composition, calorific value, absolute and envelope density, porosity, oil and grease content, presence of heavy metals, water sorption/desorption properties, and isosteric heat of sorption. Secondly, this study aims at determining the impact of such physical-chemical properties of the sludge on the MW drying performance. The MW drying performance was assessed by determining: overall sludge drying performance (exposure times to achieve a certain degree of drying), drying rates, specific energy inputs, and energy efficiencies.

2. Materials and methods

2.1. Materials and sample preparation

Three different types of WAS were obtained from three different WWTPs, while one type of SS was obtained from an onsite sanitation facility. Table 1 describes the origin of the sludge as well as the type of treatment technologies producing each particular type of sludge. All the sludge samples were stored in plastic containers at 4 °C and evaluated and/or analysed within 48 h.

2.2. Analytical procedures

2.2.1. Total solids (TS) and volatile solid (VS) determination

The TS and VS were determined according to the gravimetric methods SM-2540D and SM-2540E, as described in the Federation and Association et al. (2005). The DS% is the same as the TS concentration expressed in percentage; the moisture content was calculated subtracting the DS% to 100.

2.2.2. Calorific value and carbon (C), hydrogen (H), nitrogen (N), and sulphur (S) determinations

Carbon (C), hydrogen (H), nitrogen (N), and sulphur (S) are the main chemical elements that determine the energy content of sludge (i.e., the gross calorific value of the sludge) (Friedl et al., 2005). The gross calorific values, and the C, H, N and S content of the sludge samples were determined at the Institute of Chemistry, Ecology, Measurement and Analytics (IKEMA, Lovrenc na Dravskem polju, Slovenia) according to the following methods: (i) calorific value (SIST-TS CEN/TS 16023:2014 standard); (ii) elemental sulphur and hydrogen (Dumas method); (iii) total carbon (SIST EN 13137:2002); and (iv) total nitrogen (SIST EN 16168:2013). The gross calorific value of the sludge was determined by measuring the amount of heat emitted during the complete combustion of the sludge in a bomb calorimeter (IKA- Calorimeter C 400 adiabatisch IKA®-Werke GmbH & Co. KG, Staufen German). The gross calorific value included the condensation enthalpy of the water. The net calorific value was obtained by subtracting the condensation enthalpy from the gross calorific value.

2.2.3. N-hexane extractable material determination

The presence of N-Hexane-extractable materials (HEM), often termed as oil and grease, were determined according to the gravimetric separatory funnel extraction method suggested on the EPA Method 1664, revision B. The analysis was repeated twice, and the average of these two determinations was reported.

2.2.4. X-ray fluorescence

The X-ray fluorescence analyses were carried out to determine elements; specifically, heavy metals such as nickel (Ni), zinc (Zn), lead (Pb), chromium (Cr), and copper (Cu). The determinations were initiated by pelletizing the MW dried WAS and SS samples using a Chemplex Spectro pellet press (Chemplex Industries Inc., Palm City, USA) at a pressure of 12 tons (120 kilonewtons) in a 5 min period. The press generated sludge pellets with a radius of 16 mm and thickness of 10 mm. The concentrations of the elements (Ni, Zn, Pb, Cr, and Cu) in the pellets were determined using a Twin-X X-ray fluorescence spectrometer (XRF Twin-X, Oxford Instruments, Abingdon, UK). The spectrums were analysed by the aid of the SmartCheck software provided in the instrument.

Table 1
WWTPs and onsite sanitation facilities where the sludge samples were collected.

Sludge samples		WWTP location	Treatment technology	Wastewater/Sludge source	Mechanical pre-treatment process	Biological treatment process	Sludge treatment process
WAS	A	Ptuj	Sequential batch reactor	Industrial and domestic (80%)	Screening, grit and grease removal	Anaerobic, anoxic and aerobic	Mechanical dewatering using centrifuge assisted by the addition of polymers
	B	Ljutomer	Sequential batch reactor	Industrial and domestic (80%)	Screening, grit and grease removal	Anaerobic, anoxic and aerobic	Mechanical dewatering using centrifuge assisted by the addition of polymers
	C	Maribor	Conventional waste activated sludge	Industrial and domestic (80%)	Screening, grit and grease removal	Anaerobic, anoxic and aerobic	Saturated air flotation and mechanical dewatering using centrifuge assisted by the addition of polymers
SS	D	Ptuj	Septic tank	Domestic	Screening	Anaerobic	Gravitational draining through a sieve with an aperture size of 0.5 mm assisted by the addition of 40 mg L^{-1} cationic polymer (Acefloc 80,902+, Allied Solutions)

2.2.5. Determination of the absolute density, envelope (bulk) density, and sludge porosity

The MW dried samples were further dried in an oven at 40 °C for 72 h to reach a constant mass. The absolute density of the sludge was determined in a helium atmosphere using an AccuPyc 1330 automatic gas pycnometer (Micromeritics Inc., USA). The instrument determined the gas displaced by the sample by applying the ideal gas law and in that way the absolute volumes of the samples (and the densities) were calculated (Candanedo and Derome, 2005).

The envelope density was determined by using a GeoPyc 1360 (Micromeritics Inc., USA) instrument. The volume of the samples was analysed by packing the sample in DryFlo silica sand (registered trademark, Micromeritics Inc., USA). Then, the sample chamber of the instrument was filled with only sand and the volume of the sand was calculated. Thereafter, the sludge sample packed with the sand was introduced into the chamber, and the total volume of the sand and sludge sample was measured. From the difference in volume, the sludge sample envelope volume and density were calculated.

The porosity of the sludge was determined as the ratio of pore space volume or voids within the sample (the difference between envelope and absolute density) to the envelope volume.

2.2.6. Determination of the water sorption/desorption properties of the sludge

The determination of the water sorption and desorption properties were carried out by finding the moisture sorption isotherms (i.e., the equilibrium relationship between the moisture content of the sample at equilibrium - at the equilibrium moisture content (EMC) - and the relative humidity (RH). Such moisture sorption isotherms were determined using a dynamic vapour sorption (DVS) intrinsic apparatus (DVS Intrinsic, Surface Measurement Systems Ltd., London, UK). Two complete isotherms runs were performed for each sludge sample to capture both the sorption and desorption behavior of the material (i.e., four runs per sample). The moisture sorption isotherms were obtained for every sludge sample by plotting the moisture content of the sample (once the equilibrium was reached at each evaluated RH) as a function of the RH. The results presented in this study considered the results obtained when carrying out the second sorption/desorption run.

2.2.7. Determination of the isosteric heat of sorption

The total isosteric heat of sorption is defined as the sum of the heat change accompanying the isothermal sorption of a specified quantity of water vapour on the sludge sample (i.e., net heat of sorption), and the energy required for a normal water vaporisation (latent heat of evaporation of the unbound water). The net isosteric heat of sorption was determined as described in the Clausius-Clapeyron equation (Eq. (1)) (Poyet and Charles, 2009). The inputs for that equation were obtained using the same DVS instrument as previously described in Section 2.2.6; the net heat of sorption was calculated for each RH after the sludge sample reached moisture equilibrium. The very same procedure as described in Section 2.2.6 was followed with the sludge samples. The isotherms were carried out at two different temperatures (i.e., 25 °C and 40 °C).

$$h_{st} = Rln\left[\frac{p_1}{p_2}\right]\left(\frac{T_1 T_2}{T_1 - T_2}\right) \quad (1)$$

where h_{st} is the net heat of sorption [kJ kg^{-1}], R is the universal gas constant [kJ kg^{-1} °C^{-1}], and p_1 and p_2 [kPa] are the vapour partial pressure measured using the DVS instrument in a thermostatically sealed chamber at the two evaluated temperatures, T_1 and T_2 [°C].

The net heat of sorption is used for calculating the total isosteric heat of sorption determined according to the Eq. (2) (Sousa et al., 2016):

$$H_{st} = h_{st} + H_v \quad (2)$$

where H_{st} is the total isosteric heat of sorption [kJ kg^{-1}], and H_V is the latent heat of evaporation of pure water [kJ kg^{-1}]. The latent heat of evaporation of pure water was calculated as described in the Eq. (3) (Sousa et al., 2016):

$$H_v = 2502.2 - 2.39T \quad (3)$$

where T denotes the average temperature of the studied range (i.e., 25 °C and 40 °C). The total isosteric heat of sorption H_{st} was calculated for every RH when the sludge samples reached equilibrium regarding the moisture content. Due to the availability of the DVS instruments, only the total isosteric heat of sorption H_{st} for the WAS sample from the WWTP A was determined.

2.3. Experimental MW pilot-system

An experimental MW pilot-scale sludge drying system was designed and built for this research (Tehnobiro d.o.o, Maribor, Slovenia). A detailed schematic of the experimental pilot-scale MW system is shown in Fig. 1. The MW system consisted of a MW power supply and a MW generator delivering a maximum MW power output of 6 kW operating at a frequency of 2450 MHz. The MWs were directed to a stainless-steel drying cavity provided with a polypropylene (PP) turntable able to rotate at a speed of one rpm. The sludge samples were placed in a cylindrical PP holding vessel with a maximum sludge capacity of 6 kg. The MW generator, connected to an isolator, delivered the electromagnetic energy to the drying cavity along a standard rectangular waveguide WR340 (86.36 × 53.18 mm). A dummy water load conditioned with demineralized water at a flowrate of approximately 600 L h^{-1} was connected to the waveguide circulator used to absorb the reflected power and to prevent overheating of the MW generator. The demineralized water was used for cooling down the MW power supply. The vapour generated during the MW drying process from the drying cavity was extracted to an odour filtration system. To prevent humidity, dust, and other factors from damaging the MW generators antenna and/or the isolator, a teflon window was installed between the isolator outlet and the MW cavity's inlet. The moisture content of the sludge samples, as well as the energy consumption of the system were monitored in real-time. The changes in the mass of the sludge while irradiated (water being evaporated) was measured by a single point load cell (Mettler Toledo). The energy supplied to the pilot system was measured using a power network analyser (Etimeter, ENA3D, Poland). Kocbek et al. (2020) reported a 72% conversion efficiency of the electrical energy to the MW energy at an MW power output of 6 kW. A more detailed description of the MW pilot-system can be found in Kocbek et al. (2020).

2.4. Experimental procedure

2.4.1. MW drying tests

After determining the initial sludge moisture content of the sludge samples, three kg of each sludge sample were placed in the holding vessel of the MW system at a thickness of 60 ± 5 mm. The holding vessel containing the sludge sample was then placed on the rotating table and irradiated at an MW power output of 6 kW at a frequency of 2450 MHz. All the experiments were performed either in duplicates or triplicates. The sludge samples were irradiated until reaching a moisture content of 0.18 kg of water kg of dry solids^{-1}. The experimental conditions for the evaluated samples are summarized in Table 1. The experimental work was carried out at the research hall of the Ptuj's municipal wastewater treatment plant (Ptuj, Slovenia).

2.5. Data analysis

2.5.1. Specific energy input (SEI)

The SEI was calculated by dividing the energy input by the initial mass of sludge, as shown in Eq. (4) (Kocbek et al., 2020):

$$SEI = \frac{P_{in;elect} \cdot t}{m_{sample}} \quad (4)$$

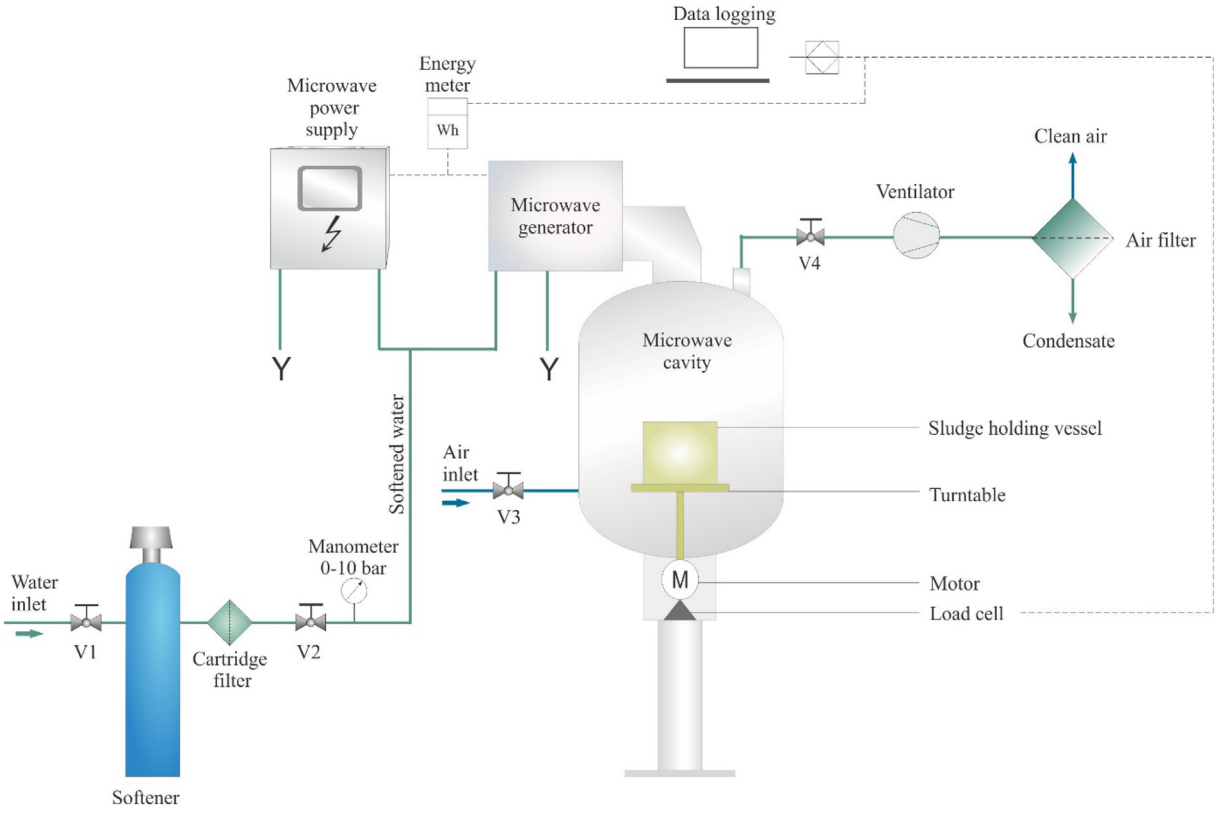

Fig. 1. Schematic representation of the experimental pilot-scale MW system (Kocbek et al., 2020).

where the SEI is the specific energy input [kJ kg^{-1}], m_{sample} is the initial mass of sludge (kg), t is the exposure time [s], and $P_{in;elect}$ is the input power consumed by the system during the drying process [kW]. The SEI has been previously used and explained in Kocbek et al. (2020).

2.5.2. Energy efficiency (μ_{en})

The μ_{en} is the ratio between the theoretical energy demand for evaporating the water and the energy consumed by the MW unit during the drying process, the calculation for which is shown in Eq. (5) (Jafari et al., 2018):

$$\mu_{en} = \frac{(m_{sample} \cdot c_p \cdot \Delta T) + (m_{eva} \cdot H_V)}{P_{in;elect} \cdot t} \cdot 100 \quad (5)$$

where μ_{en} is the energy efficiency [%], c_p is the specific heat capacity of the water [J kg^{-1} $°C^{-1}$], ΔT is the temperature difference of the sample between the exposure time t and the start of the treatment, and m_{eva} is the amount of evaporated moisture (water) [kg]. The temperature of the samples was not measured; as such, the influence of sensible heat on total energy efficiency was considered assuming the sludge sample reached a temperature of 100 °C before water evaporation took place (i.e. at the end of adaptation drying periods estimated from the Krischer's drying curve) (Radomski et al., 1978; Kocbek et al., 2020).

2.5.3. Sludge moisture content (X)

The X was calculated as shown in Eq. (6) (Chen et al., 2014):

$$X = \frac{m_t - m_d}{m_d} \quad (6)$$

where *X* is the moisture content of the sludge [kg of water per kg of dry $solid^{-1}$], m_t is the sample mass [kg] at time t and m_d is the total mass of dry solids in the sample [kg]. The total mass of dry solids in the samples was determined as described in Section 2.2.1. The m_t was continuously determined by the point load cell located in the MW irradiation cavity, as described in Section 2.2.1. Therefore, X was continuously measured.

2.5.4. Drying rate (D_R)

The D_R was calculated as shown in Eq. (7) (Chen et al., 2014):

$$D_R = \frac{dX}{dt} \quad (7)$$

where D_R is the drying rate [kg of water per kg of dry $solid^{-1}$ min^{-1}] and X is the moisture content of the sludge at a specific exposure time. The drying rates were determined by polynomial regression analysis using Microsoft Excel and considered at a mass interval of 20 g.

2.5.5. Power absorption density

According to Maxwell equations, the power absorption density (i.e., the amount of power absorbed by a material per unit of volume) (P_d) is proportional to the input power, which relates to the electric field intensity (E), as shown in Eq. (8) (Stuerga, 2006); Gupta and Leong (2007):

$$P_d = 2\pi f \varepsilon_0 \varepsilon' |E|^2 \quad (8)$$

where P_d is the amount of absorbed power per unit volume [Wm^{-3}], *f* is the MW frequency [s^{-1}], ε_0 is the permittivity of free space [8.85×10^{-12} fm^{-1}] and E is the electric field intensity [Vm^{-1}]. The electric field intensity can be calculated as described in Eq. (9) (Soltysiak et al., 2008; Pitchai et al., 2012).

$$E = \sqrt{\frac{2P_{out,micr}}{1 - |S_{11}|^2}} \quad (9)$$

where $P_{out;micr}$ is the output power (nominal power) supplied to the MW chamber [kW] and, S_{11} is the reflection coefficient associated with the fraction of the power reflected by the sample.

Assuming that the absorbed MW energy is converted into heat, the heating rate during the MW drying process can be related to power absorption density as follows (Clark et al., 2000; Beneroso et al., 2017):

$$\beta = \frac{P_d}{\rho c_p} \tag{10}$$

where β [°C s^{-1}] is the heating rate (i.e., the temperature variation of the material with time) and ρ is the material density [kg m^{-3}].

3. Results and discussion

3.1. Sludge physical-chemical characteristics

The physical-chemical characteristics of the evaluated sludge from the different sources and treatment facilities are depicted in Table 2. The average initial moisture content of the sludge samples evaluated in this study ranged between 79.6% and 84.3%. The moisture content of the WAS samples A, B and C was on average 81 ± 1.5%. That reflects the good performance exhibited by the mechanical dewatering unit (i.e., centrifuge) on the sludge dewatering. Similar values were reported in the literature, with sludge moisture content ranging between 79 and 87% (Léonard et al., 2004; Mawioo et al., 2017). The effectiveness of the conditioning methods for dewatering the SS samples were also effective as reflected in the SS moisture content of 84.3%. The SS (sample D) samples were flocculated, dewatered by gravity, and sieved.

The organic content of the evaluated samples (expressed as VS) shown in Table 2 ranged between 68 and 88%. Such variability could be eventually explained due to either the inherent properties of the different types of evaluated sludge, or to the treatment processes the sludge went through. The VS concentrations of the WWTP A, B, and C were similar with an average VS concentration of 86 ± 4%. The lowest VS fraction was obtained for the sludge sample D at a VS concentration of 68%. This value could be eventually attributed to the long sludge holding time of the sludge (five years or longer) at the storage SS tank in the WWTP; thus, the degradation of some of the organic material could occur. Considering such long retention time at which the SS was exposed and the subsequent reduction in the VS concentration, it was also expected a potential reduction on the gross calorific value of such SS. However, as shown in Table 2, the gross and net calorific values of the SS (sample D) were comparable with the values obtained for the WAS samples A, B, and C. Average values for the gross and net calorific values of 19 ± 0.5 MJ kg^{-1} and 17.3 ± 0.6 MJ kg^{-1}, respectively were obtained for the evaluated samples. Therefore, there were no major variations on both the gross and net calorific values considering the large variations on the VS concentrations. In addition, the C, H, N, and S content of the different samples (WAS vs SS) did not change considerably. Average concentrations for C, H, N, and S of 43.6 ± 3.2%, 5.3 ± 0.4%, 7.2 ± 3.1%, and 1.5 ± 0.1%, respectively were reported for all the evaluated samples. The high calorific value obtained for the SS (sample D), could be then attributed to the higher oil and fat content reported for the SS samples compared to the WAS samples (1.36 g gDS^{-1} for the SS compared to a range from 0.28 to 0.35 g gDS^{-1} for the WAS sludge samples). The SS samples were obtained from septic tanks receiving household wastes that could have included waste cooking vegetable oil, and similar products with a high oil and grease content. As such, the high oil and grease content on the SS samples could have exhibited a positive effect on the SS samples regarding their energetic value. For instance, the amount of heat released during the combustion of waste cooking vegetable oil is higher than 40 MJ kg^{-1} (Fassinou, 2012). So, when vegetable oils were present in the sludge matrix, the calorific values observed in sludge samples could increase.

The sludge flock structure is usually porous and contains voids through which the fluids (i.e., water) can move through (Cui et al., 2019). The porosity values for the evaluated samples are reported in Table 2. The porosity of the evaluated sludge samples ranged between 43 and 64%. Higher porosity values were observed for the SS (sample D) than for the WAS sludge samples. That could be eventually attributed to the large retention time at which the SS was retained in the storage tanks eventually promoting the degradation of sludge. Following the Kozeny – Carman equations, the higher the porosity, the higher the permeability of the sludge; thus, the higher the potential dewaterability of the sludge (Schulz et al., 2019). Therefore, the SS (D) could eventually exhibit a higher tendency for loosing water compared to the other sludge samples. In other words, high permeable-porous media may induce a higher driving force and accelerate the flow through the sludge matrix, whereas low permeability porous media decelerates such flow. Therefore, the SS (D) could eventually exhibit a higher tendency for loosing water compared to the other sludge samples. However, other factors should have been also considered such as the type and dose of conditioning agents used for the flocculation and coagulation process, the dewatering implemented procedure (which could all affect floc morphology), the specific surface area, and the fractal dimension (Feng et al., 2019; Schulz et al., 2019), which were not evaluated in this study. For instance, Feng et al. (2019) reported that organic flocculants increase the floc particle size, decrease the specific surface area, and decrease the fractal dimension; whereas the fractal dimension gradually decreased as the inorganic flocculant dosage was increased having a more substantial effect on the sludge permeability. Accordingly, the sludge permeability was favoured when applying inorganic flocculants (Feng et al., 2019). In addition, the high level of organic matter in the municipal sludge compared to

Table 2
Physical-chemical characteristics of the evaluated sludge samples.

Parameter	Unit	Sample A	Sample B	Sample C	Sample D
Moisture content	[%]	83 ± 1.0	79.6 ± 0.2	80.0 ± 0.1	84.3 ± 0.2
Dry solids	[%]	17 ± 1.0	20.4 ± 0.2	20.0 ± 0.1	15.7 ± 0.2
Volatile solids	[%]	88 ± 2	81 ± 0.2	88 ± 0.3	68 ± 1.2
C	[%]	46.5	39.8	46.1	42.0
H	[%]	5.0	5.5	5.7	4.8
N	[%]	9.9	9.3	6.51	3.2
S	[%]	1.5	1.5	1.3	1.5
Gross calorific value	[MJ kg^{-1}]	18.4	19.0	19.6	18.9
Net calorific value	[MJ kg^{-1}]	16.7	17.3	17.9	17.2
Oil and grease	[g gTS^{-1}]	0.35 ± 0.01	0.31 ± 0.003	0.28 ± 0.16	1.36 ± 0.04
Absolute density	[g cm^{-3}]	(141 ± 0.13) × 10^{-2}	(144 ± 0.05) × 10^{-2}	(141 ± 0.04) × 10^{-2}	(149 ± 0.05) × 10^{-2}
Absolute volume	[cm^3]	(405 ± 0.36) × 10^{-2}	(342 ± 0.11) × 10^{-2}	(284 ± 0.09) × 10^{-2}	(178 ± 0.05) × 10^{-2}
Envelope density	[g cm^{-3}]	(80 ± 0.50) × 10^{-2}	(80 ± 0.50) × 10^{-2}	(71 ± 0.40) × 10^{-2}	(54 ± 0.50) × 10^{-2}
Envelope volume	[cm^3]	7.16	6.13	5.67	4.97
Porosity	[%]	43	44	50	64
Nickel (Ni)	[mg kg^{-1}]	23.2	57.9	19.7	22.4
Zinc (Zn)	[mg kg^{-1}]	437	1403	524	872
Lead (Pb)	[mg kg^{-1}]	25	71	29	45
Chromium (Cr)	[mg kg^{-1}]	68	2981	51	82
Copper (Cu)	[mg kg^{-1}]	55	70	75	61

in the septic sludge, as well as the dewatering strategy (Table 1), result in a compression of the sludge; that could also lead to an enclosure of drainage channels in the municipal sludge body due to the high mechanical pressure during the squeeze process. Hence, having an important effect on the sludge porosity (Collard et al., 2017; Zhang et al., 2019b).

The results of the X-Ray fluorescence of the sludges sample are provided in Table 2 and as supplementary material to this paper [see Fig. S1]. The concentrations of metals present in the sludge samples including Ni, Zn, Pb, Cr, and Cu complied with the European standards for agricultural reuse of 400 mg kg^{-1} for Ni, 4000 mg kg^{-1} for Zn, 1200 mg kg^{-1} for Pb, and 1750 mg kg^{-1} for Cu (Wiśniowska et al., 2019). However, most European countries adopted more stringent regulations with respect to land applications of treated sludge. For instance, the Slovenian regulation for sludge reuse in agriculture set the following standards: 30 mg kg^{-1} for Ni, 100 mg kg^{-1} for Zn, 40 mg kg^{-1} for Pb, 40 mg kg^{-1} for Cr, and 0.5 mg kg^{-1} for Cu (Wiśniowska et al., 2019). These results indicated that the potential agricultural reuse of the treated sludge derived from WWTP and SS tanks would significantly vary depending on the local regulations. Nevertheless, sludge not suitable for agriculture, can be alternatively converted into stable fractions through (co-) combustion, while generating heat and electricity. In such circumstances, the sludge needs to be transported from WWTP to centralized incinerations plants requiring higher sludge transportation costs compared to the reuse of such sludge in agricultural applications. For instance, Slovenia has approximately 250 municipal WWTPs in operation; however, only 10% of such facilities have a treatment capacity larger than 10,000 PE (LeBlanc et al., 2009). Similar situations are observed in other European countries (Ledakowicz et al., 2019). In such cases, it is not economically feasible to implement in-situ advanced sludge treatment processes to locally deal with the sludge. In such circumstances, the sludge needs to be transported to centralized treatment/disposal sites requiring high sludge transportation costs; thereby, emphasizing the importance of implementing strategies to reduce sludge mass and volume at the WWTPs.

Fig. 2 depicts the adsorption/desorption behavior of the MW dried sludge samples (moisture sorption isotherms). For all the evaluated samples, similar shapes on the sorption isotherms were obtained with an initial low water sorption/desorption at low RHs, and a substantial increase at high RHs (above 75%). The curves indicates an S-shape, commonly observed in organic materials, such as sludge (Vaxelaire, 2001; Freire et al., 2007) and provides an insight into different water-binding mechanisms at the individual sites of the sludge (Mujumdar and Devahastin, 2000). Several models have been proposed to explain the shape of the sigmoid sorption isotherm shown in Fig. 2. Hailwood and Horrobin (1946), suggested that water adsorbed onto the sludge exist in two forms: (i) water of hydration, corresponding to the water molecules bound to the OH groups in the sorbent material (sludge in this case) by polar interactions (monolayer water); and (ii) solid solution or dissolved water, corresponding to the water molecules slightly bound to the sorbent material, but still located within the porous structure of the sludge (poly-layer water). As a result, the strength of the water molecules bound to sludge during the sorption/desorption processes would depend on the presence and availability of hydrophilic and polar groups responsible for producing strong intermolecular interactions between the water molecules and the sludge. From looking at Fig. 2, three different regions can be distinguished, which may eventually indicate different binding characteristics between the water molecules and the sludge. The first region can be observed at low RH (left side of Fig. 2 towards the first bend, from 0 to approximately 20%). In that region, it seems that is more difficult for the water molecules to get adsorbed/desorbed in the sludge matrix. The water molecules may interact with the hydrophilic groups of the material such as the OH or NH groups (Peleg, 2020). This was described as the type (i) interaction and/or monolayer adsorbed water. Thus, the lower part of the isotherm is characterized by water molecules tightly bound to the sludge. The enthalpy of evaporation for that type of water as described in that region has been reported by other authors to be much higher than that of pure water confirming such strong bonding between the water molecules and the sludge (Andrade et al., 2011).

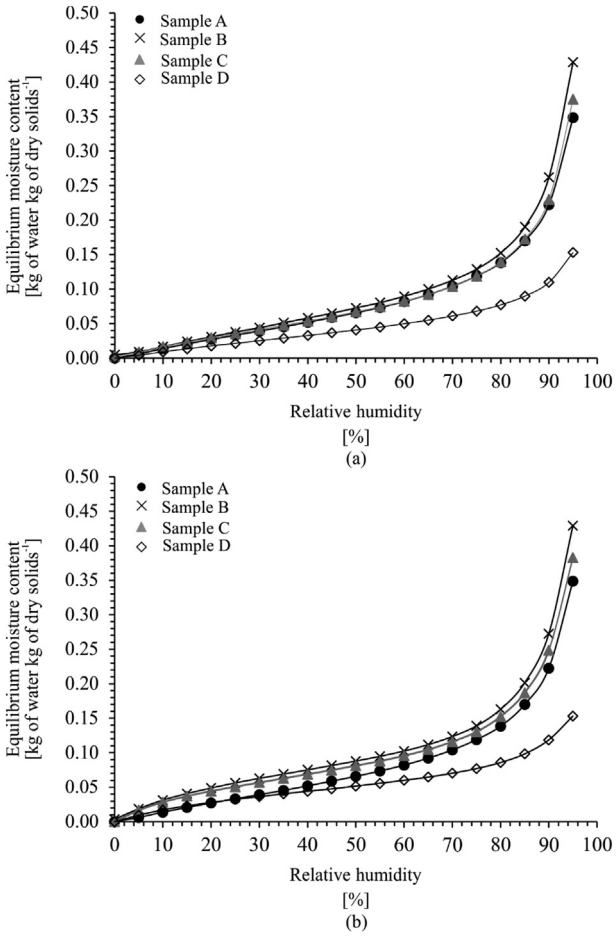

Fig. 2. Equilibrium moisture content (EMC) as a function of the RH (moisture sorption/desorption isotherms) for the evaluated sludge samples during (a) adsorption and (b) desorption.

In the second region (between the first (20%) and second bends (75%)), the slope of the curve is higher than in first region and the water molecules seemed to be less tightly bound to the sludge compared to the first region. In this region eventually different layers of water could form one on top of each other (that is, on top of the first monolayers) (Bougayr et al., 2018). The enthalpy of evaporation for the water molecules in this zone has been reported by other authors to be slightly higher than that of pure water (Penfield and Campbell, 1990; Andrade et al., 2011). In the third region (above the second bend, above 75%), the slope becomes steeper and the water molecules seemed to be loosely bound; mainly the water molecules can be adsorbed in cavities in the sludge matrix, in large capillaries, and in sludge voids (Penfield and Campbell, 1990; Andrade et al., 2011). As the RH increased, the sludge cavities and voids seemed to become increasingly occupied. Then, the absorption of the water molecules could occur onto less active sites involving lower interaction energies. When the RH approaches 100%, the curve leans to a vertical asymptote, which represents the free water present in the sludge (Bougayr et al., 2018). In conclusion, the intermolecular forces between the water molecules and the sludge observed at the lower RHs (characterized by the presence of adsorption active sites in the sludge such as OH or NH groups - monolayer adsorption) were much stronger that the forces involved in the interaction between the water molecules and the sludge at higher RHs (characterized by the water bound to the sludge cavities and voids - multilayer adsorption). Correspondingly, the amount of energy that must be supplied to the material during desorption (drying) would strongly depend on the characteristics of the molecular bonding between the water and the sludge.

As observed in Fig. 2, the different sludge samples showed different affinities for adsorbing/desorbing water at the evaluated RHs. The SS (sample D) showed the lowest EMCs at the evaluated RHs. The WAS samples (samples A, B, and C) exhibited similar EMCs at the entire evaluated RHs, slightly higher than for the SS (sample D). For instance, at a 95% RH (Fig. 2a), the SS (sample D) reached the lowest EMC value of 0.15 kg of water kg of dry solids^{-1}, compared to the WAS sample A (0.35 kg of water kg of dry solids^{-1}), WAS sample C (0.38 kg of water kg of dry solids^{-1}), and WAS sample B (0.43 kg of water kg of dry solids^{-1}). The SS (sample D) was characterized by the lowest amount of moisture content; so, the less amount of bound water. Therefore, the highest amount of free water. That is, assuming that the EMC values at RH of 95% represents the free water content of the sample; then, the free water content in the sludge samples A, B, C, and D were 69, 62, 65 and 84%, respectively. This could be eventually related to the organic and oil and grease content in the sludge; these values were presented in Table 2. The SS (sample D) contained a much lower concentration of organic matter compared to the WAS samples; thus, less available sites for the water molecules to get adsorbed. In addition, oil and grease compounds are highly hydrophobic having a significant effect on the uptake of water from the environment; consequently, resulting in low EMC values. As indicated both in Fig. 2 and Table 2, there is inverse relation between the EMC and the oil and grease content in the sludge; that is, the higher the oil and grease concentration in the sludge, the lower the EMC values. Thus, the presence of oil and grease together with a low organic matter content seemed to increase the hydrophobicity of the sludge. Having such high hydrophobicity is a desirable property of a material when the goal is to dry such material. Therefore, sludge samples with such high hydrophobic (as SS – sample D) would eventually exhibit a better performance when exposed to MW drying.

The isosteric heat of sorption provides an indication of the strength of the interaction between the water molecules and the material. In this study, the isosteric heat of sorption was assessed for the WAS sample A at a sludge moisture content ranging from 0.01 to 0.38 kg of water kg of dry solids^{-1} following the same procedure as for obtaining the moisture sorption isotherms described in Fig. 2. As shown in Fig. 3, the isosteric heat of sorption decreased as the sludge moisture content increased in the evaluated sludge moisture content range; in addition, the isosteric heat of sorption at the entire sludge moisture content evaluated range was always higher than the heat of evaporation of pure water (2.4 MJ kg^{-1}). These results clearly indicate that the lower the moisture content in the sludge, the higher the energy required to remove that water from the sludge. That is, the lower the moisture content the higher the presence of water molecules bound to the sludge to polar sludge active sites such as the OH and NH groups (monolayer water), so higher amount of energy would be required to break such water bonding. As the sludge moisture content increased, the energy required to remove the water out of the sludge decreased. Therefore, it is expected that the energy required by a MW system for drying such type of sludge would increase as the sludge moisture content decrease. In this study the isosteric heat of sorption was only determined for the WAS sample A, but it was not determined for the other sludge samples. However, looking at the moisture sorption/desorption isotherms presented in Fig. 2, no majors differences on the isosteric heat of sorption are expected between all the evaluated sludge samples; eventually, the SS sample D would exhibit a little lower isosteric heat of sorption compared to the other sludge samples.

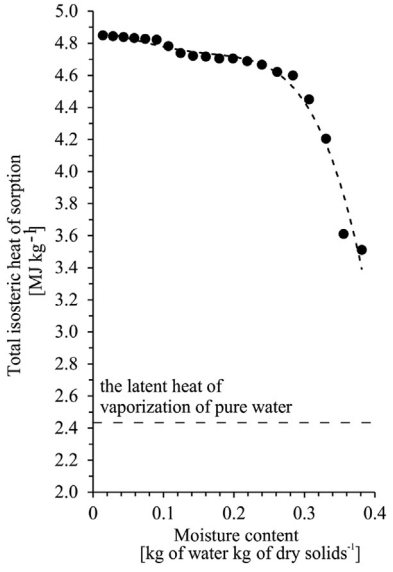

Fig. 3. Isosteric heat of sorption as a function of moisture content.

3.2. Sludge MW drying: drying rate performance

Fig. 4 shows the changes in the moisture content of the evaluated sludge samples as a function of the exposure times. Fig. 5 indicates the changes in the drying rates of the sludge samples as a function of the exposure time (Fig. 5a) and moisture content (Fig. 5b). Similar shapes were observed for the four evaluated sludge samples; however, sludge samples D and A clearly contained a higher initial moisture content. Three different drying periods can be clearly observed in Fig. 5 as follows: (i) the adaptation drying period, (ii) the constant rate drying period, and the (iii) the falling rate drying period. At an early stage of drying process in the adaptation drying period, the temperature of the sludge raised until the vapour pressure of the evaporated water is equal to the surrounding pressure. The water in the sludge sample evaporated at the atmospheric boiling point (100 °C) (Doran, 2013; Berk, 2018). As the temperature increased, the drying rates also increased. The maximum drying rate indicated the end of the adaptation phase and the beginning of the constant rate drying period. Notably, the higher the initial moisture content of the sludge samples (Fig. 4), the higher the maximum drying rates observed in Fig. 5. A reduction in the moisture content of the sludge samples of approximately 23% was observed in the adaptation period. Following the initial adaptation drying rate period, a steady state drying rate was achieved. During that period, the water evaporated consisted of the free water present in the surface of the sludge. The constant drying period lasted as long as the water transportation rate from the inner part of the sludge to the surface was equal or higher than the water evaporation rate from the surface of the sludge (Doran, 2013; Berk, 2018). The constant rate drying period lasted for a considerable large amount of time, almost until the drying process was finished. This observations are in agreement with previous studies reported in the literature (Dominguez et al., 2004; Chen et al., 2014; Bennamoun et al., 2016; Mawioo et al., 2017; Kocbek et al., 2020). Dominguez et al. (2004) reported that MW dryers extended the duration of the constant rate drying period

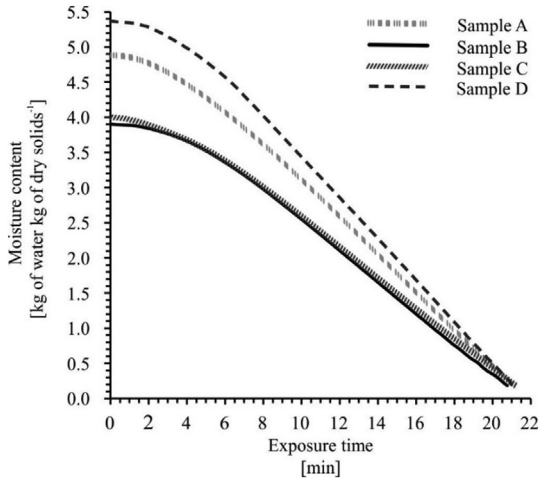

Fig. 4. Moisture content as a function of the exposure time for the evaluated sludge samples.

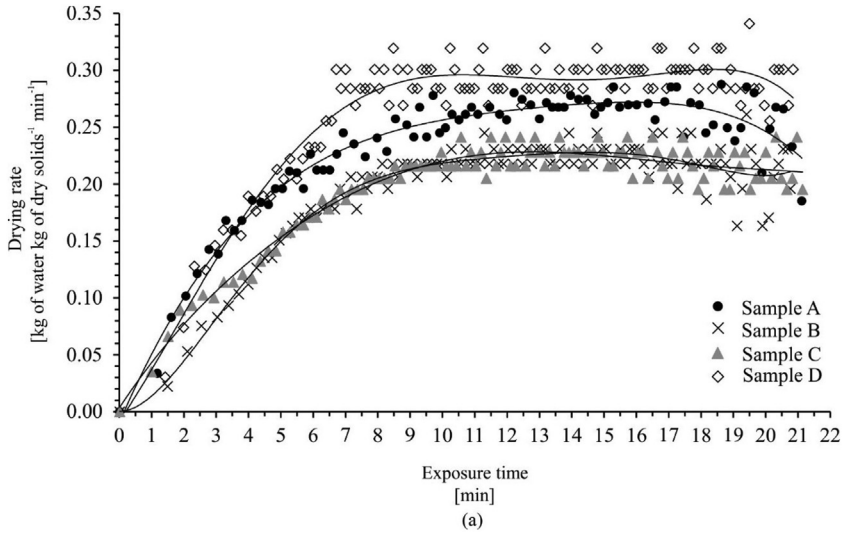

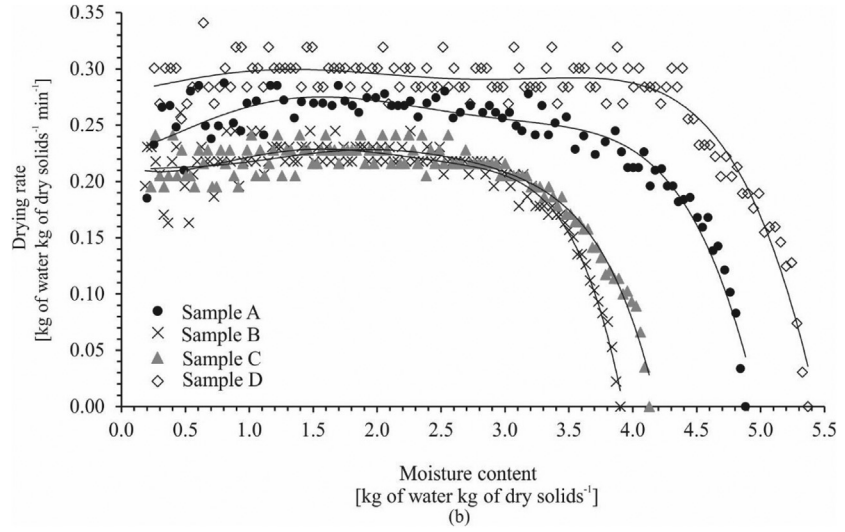

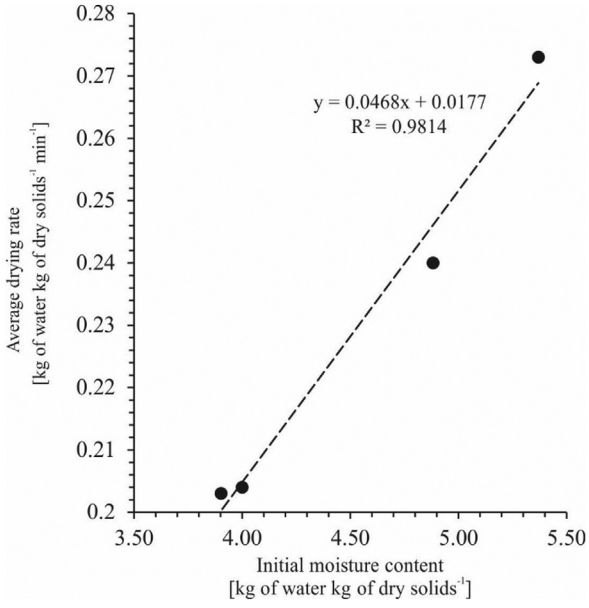

Fig. 5. Drying rates as a function of the (a) exposure time, (b) moisture content and (c) initial sludge moisture content.

compared to traditional conductive and convective dryers. Ni et al. (1999) and Fu et al. (2017) observed that the increase in the constant drying rate periods (i.e. removal of free and loosely bound water) could be attributed to the selective penetration of the MW irradiation to certain absorbent materials; therefore, causing heat generation from the inside of the target material creating an inverted temperature profile compared to conventional dryers (i.e. in MW irradiation the temperature is higher inside the material rather than in the surface of the material). This heat, a result of molecular friction, causes internal evaporation which in turn increases the internal pressure promoting the water mass transfer to the surface of the material. Such process accelerates the drying rates and extends the constant drying rate period in MW drying. As the drying process continued, the sludge moisture content of the sludge samples further decreased, and the drying rates started to fall. At that point, the process reached the falling drying rate period. At the start of the falling rate period, the amount of the free water in the surface of the sludge declined; the liquid film on the surface of the solid is no longer present (Doran, 2013; Berk, 2018). This condition is gradually expanded until the surface of the material is completely dry. So, the drying process continued, but the evaporating surface moves into inside the material becoming harder than before to transfer the moisture from the capillaries and interstices of the material to the surface (Doran, 2013; Berk, 2018). As such, the drying rate decreased since the water removal process was now being governed by internal diffusion mechanisms (much slower than the evaporation of the free water). The start of such falling drying rate period also indicated the end of the free water removal, and the start of the bound water removal. The sludge samples were dried up to 15% moisture content. A prolonged exposure of the sample to the MW irradiation would have resulted in a longer and more notable falling drying rate period as reported by Bennamoun et al. (2016) and Chen et al. (2014). An interesting observation from looking at the results in Fig. 5, is that the drying falling rate period was attained faster in sludge samples from the centralized WWTP (A, B and C) compared to the sludge sample taken from the septic tanks (D); thus, confirming that sludge sample D contained less bound water compared to WAS samples (as discussed in Section 3.1). In conclusion, the concentration of organic matter in the sludge, as well as the presence of oil and grease have an impact on the MW drying performance of the sludge. The results presented in this section validated that MW irradiation accelerated the evaporation of water from the surface of the material, while extending the duration of the constant drying rate period. This allowed the unbound water to be removed regardless the type of sludge being evaluated.

In addition, Ma et al. (2017) and Antunes et al. (2018) reported that the rate of the water evaporation (from the sludge surface when applying MW radiation) was influenced by the rate at which the electromagnetic energy is absorbed by the material and converted into heat (power absorption density (P_d)). This has been reported to largely depend on several factors including both the electric field strength (which depends on the MW power output), as well as the dielectric properties of the sludge such as the dielectric loss factor (ε'') as described in Eq. (8); particularly, the sludge moisture content directly impact on the dielectric loss factor (ε'') (Ma et al., 2017; Antunes et al., 2018). For instance, Ma et al. (2017) reported dielectric loss factor (ε'') of 14.1 for municipal dewatered sludge at a moisture content of approximately 81%. As the sludge was dried (i.e. as the water content of the sludge was reduced) up to a sludge moisture content of 6%, a the dielectric loss factor (ε'') of 0.3 was reported (Ma et al., 2017). Similar values were also reported by Antunes et al. (2018). However, the authors reported that the impact of the moisture content on the MW performance depended also on other parameters beyond the dielectric properties of materials such as the MW field intensity, and power conversion capacity, among others. That is, the moisture content of the sludge has a direct impact on the dielectric loss factor; therefore, on the power absorption density (P_d – as described in Eq. (8)), and on the rate at which the MW electromagnetic energy is absorbed into the sludge samples. The water molecules strongly interact with the applied MW field. So, the higher the moisture content (i.e., the higher the power density), the higher also the heating rate β as described in Eq. (10); that is, the higher the rate at which the temperature of the sludge increases. In other words, a material with a high moisture content would absorb more MW energy, leading to a faster warm-up and a higher internal vapour pressure gradient compared to a low moisture content material removing the moisture from the material at a faster rate (Ni et al., 1999; Kumar et al., 2016). Other authors also agree with such observation (Ni et al., 1999; Du et al., 2005; Zhang et al., 2016; Zhang et al., 2019a). Such trends were clearly observed in this study. Fig. 5 c shows that average drying rates increased linearly when increasing the initial sludge moisture content. The sludge sample with the highest moisture content (SS sample D – Fig. 4) exhibited the higher drying rates (Fig. 5). Such higher drying rates observed for the sludge samples with a higher moisture content, allowed the same exposure time required for all the samples to reach a final moisture content to 0.18 kg of water kg of dry solids^{-1} as shown in Fig. 4, regardless the initial moisture content of the water. The exposure time needed to dry the sample up to 0.18 kg of water kg of dry solids^{-1} was similar across the entire range of evaluated sludge samples at an average of 21 ± 0.4 min (Figs. 4 and 5). In other words, despite the fact that the initial moisture content of the SS sample D exposed to MW irradiation required a higher energetic demand (higher specific heat capacity), it was dried in a similar exposure time. The SS required less energy to be dried than the other sludge samples due to the pressure driven flow induced in the SS sludge by a more efficient absorption of the MW energy within materials provided with a higher initial moisture content than the other sludge samples. Other authors have observed similar trends, but also reported that the favourable conditions for the absorption and conversion of MW energy into heat, observed at a higher sludge moisture content, could also be counteracted by the higher net amount of water initially present in the sludge sample that needed to be removed to reach the desired drying goal (Du et al., 2005). Therefore, the increase in the dielectric properties of the irradiated material does not necessarily means lower exposure time for achieving a desired level of moisture content. The latter may be perhaps observed when considering sludge material with a greater difference on the initial moisture content.

According to Jones and Or (2003), both the free and loosely attached water molecules to the material exhibit low physical attractions to the material and can move more freely compared to the bound water. Hence, such water molecules can be easily rotated under the oscillating electromagnetic field provided by the MW irradiation; so, resulting in friction and heat. On the other hand, the effective movement of the bound water molecules is constrained by the strong physical binding forces between the solid material and the water molecules. Consequently, those water molecules cannot effectively absorb and convert the energy generated by the kinetic movements into heat; therefore, resulting in lower drying rates (Jones and Or, 2003). Such water fractions of the sludge (free and bound) can vary considerably depending on the source of the wastewater and the treatment processes at which the sludge was subjected to. The amount of bound water present in the sludge was determined in this study by assessing the water sorption isotherms of the MW dried sludge (shown in Section 3.1). The SS sludge (sample D) exhibited the lowest amount of bound water in the sludge compared to the WAS samples (A, B and C). Thus, the SS (sample D) (exhibiting an initial high water moisture content) could have absorbed the MW energy more efficiently leading to the higher drying rates shown in Figs. 4 and 5. In additions, due to the higher free water content of the SS (sample D), longer constant drying periods were observed for these samples as shown in Figs. 4 and 5 compared to the WAS samples. Therefore, the results presented in this section demonstrated that the quantity and the distribution of water within the sludge matrix have a substantial impact on the MW sludge drying performance by affecting the absorption and conversion of MW energy into heat. Specifically, the sludge samples characterized with a higher amount of free and loosely bound water promoted a higher MW energy absorption and conversion of energy into heat leading to higher drying rates and to the extension of the constant drying rate duration.

Furthermore, the higher the oil and grease content of the sludge, the higher the amount of free or loosely bound water in the sludge; that is, the higher the hydrophobicity of sludge. The presence of oil and grease materials in the sludge (e.g., fats and oils) could also positively impact the

thermal conductivity and specific heat capacity of the sludge (Lyng et al., 2014). Oil and grease materials exhibit higher thermal conductivities and lower specific heat capacities than water; thus, requiring less energy for rising the temperature of the heated material (Lyng et al., 2014). Therefore, the presence of oil and grease components in the SS (sample D) (showing the highest oil and grease concentrations compared to the other sludge samples – Table 2) could also contribute to the high drying rates observed for the SS (sample D) compared to the other sludge samples (Figs. 4 and 5). For instance, Das and Rajkumar (2011) evaluated the effects of various fat concentrations (5, 10, 15, and 20%) on treating cooked goat meat patties. Each patty was heated using MW to an internal temperature of 75–80 °C (700 W, 2.45 GHz). The results showed that the MW cooking time decreased with an increase in the fat content. The latter has been attributed to a decrease in the dielectric constant and loss factor with the increase in the fat content. The fat and oil content were also greatly reported to affect the heating uniformity. Consequently, the amount of fat present in the sludge material not only have an effect on the sludge hydrophobicity (Section 3.1) (and leads to prologued constant drying period (Section 3.2) associated with high drying rates), but could also positively affects the MW heating in terms of the heating rate and the temperature uniformity. That could lead to shorten the exposure time; thus, lowering the energy demand to treat the material. Therefore, the fats and oil might have contributed to: (i) a decrease in the bound water content observed in the SS sample D compared to the WAS samples; and (ii) the provision of a more uniform temperature uniformity through the body of the samples resulting in faster drying rates having a positive effect on the sludge drying process.

Other compounds present in the sludge samples, such as the organic matter content could also influence the sludge drying process. That is, the higher the organic content of the sludge, the more water can be bound to the sludge matrix requiring more energy to be removed. Likewise, other physical-chemical properties such as the porosity and permeability could promote faster MW drying rates by providing better possibilities for the water molecules and water vapour to diffuse out of the material (Pickles et al., 2014). In other words, the electrical conductivity and thermal conductivity of the sludge depends on the material porosity, pore radius, and fractal dimension (Macías-García et al., 2020). Therefore, the pore structure in the MW irradiation process will influence the dielectric properties and the power absorption of energy by the exposed material to the MW irradiation during the drying process. The porosity of sludge could also continuously change during the sludge drying process. Specifically, the application of thermal processes to sludge leads to the evaporation of water molecules present in the sludge pores, causing a vapour pressure gradient that might have an important effect on the pore evolution. As such, resulting on the possible formation of new cavities and openness in the dried sludge; in addition, the porosity, surface roughness, and the specific surface area of the sludge could also be modified during the drying process (Feng et al., 2014). All of which have a substantial effect on the material and could have favoured the increase of the SS sludge sample porosity and permeability; therefore, lowering the resistance for removing the moisture present in the pores through the interior pore channels of the solid's materials (Yiotis et al., 2010). In other words, the SS sample (D) as shown in Table 2 also exhibited the highest porosity values compared to the other evaluated sludge, so that could probably also contribute the highest drying rate observed for the SS.

These results indicate that the MW drying performance strongly depend on the sludge physical-chemical properties determined and presented in this study such as the moisture content, the porosity, the organic matter content (VS content), the oil and grease content, and the type of interaction between the water molecules and the sludge, among others. These properties exhibited a strong influence on the MW drying performance for the treatment of sludge, and the better these properties are known, the better the performance of the MW drying system can be predicted. Notably, the MW drying and energy performance vary according to the parameters determined in this study such as the organic content, fat and oil content, the presence of heavy metals, and other constituents of the sludge matrix. Despite the fact that the selected physicochemical parameters and experimental procedure used in this research provided new information and interesting findings, there is still a gap in the knowledge that needs to be further explored to provide a better understanding of the interaction between the MWs and the sludge matrix. This interaction could have a substantial influence on the system throughput capacity; thus, on the design and performance of the MW drying system. Therefore, further research would be needed to assess the impact of the physicochemical properties of sludge on the dielectric properties of sludge as a function of the drying exposure time; in addition, the mechanisms occurring during the drying process (heat and mass transfer processes) need to be better understand with respect to MW drying. Several other properties of sludge (e.g., porosity, thermal conductivity, permeability and others) should also be better examined to better understand the sludge drying performance when using MW irradiation.

The effect of the sludge properties such as the volatile solids content have a more evident impact on conventional drying techniques such as conductive and convective methods than in MW drying. Léonard et al., (2004) reported drying rates varying from 0.96×10^{-3} to 1.96×10^{-3} kg of water m^{-2} min^{-1} when drying sludge with similar moisture content (84 ± 3%) using convective methods (hot air). The lowest drying rates, so the highest drying times, were observed when treating the sludge with the highest content of volatile solids (i.e., organic content). Whereas, in the present study the difference in exposure time needed to dry the different sludges were marginal (21 ± 0.4 min). Accordingly, for conventional drying processes it is difficult to determine the length of the individual drying periods. The drying periods could be strongly affected by the properties of the sludge and the external condition, as the drying process using traditional drying approaches is mainly influenced by the moisture transport mechanisms inside the material to be dried (i.e., falling drying rate period) (Léonard et al., 2004; Tao et al., 2005; Li et al., 2016; Kocbek et al., 2020). The design and scale-up of most conventional dryers are commonly preceded by laboratory and/or pilot scale evaluations with reference to the specific material being processed. On the other hand, this research demonstrated that for MW drying the initial moisture content had a governing impact on the sludge drying performance. Therefore, the design calculations could be potentially simplified. In addition, the fluctuation in sludge composition, will not have a substantial effect on the operation of the MW system throughput capacity. However, the different types of sludge in this research were treated up to a final 15% moisture content (85% DS); an increase in the mass and heat transfer resistance may be observed at lower moisture content. Thus, eventually influencing the design aspect and operation of the MW dryers considerably.

3.3. Sludge MW drying: energy performance

The energy performance of the MW system was also evaluated in terms of both the energy efficiency μ_{en} (Eq. (5)), and the actual MW energy consumed for drying the sludge samples until the desired (final) moisture content (defined as the SEI as described in Eq. (4)). One alternative for measuring the energy efficiency performance of a drying system is to look at the ratio between the latent heat of the water and the actual energy consumed during the drying process (Earle and Earle, 2004). However, as described in Eq. (5), in this study the sensible heat was also factored (in addition to the latent heat) as it can be possible to recover that energy as heat. Both the energy efficiency (μ_{en}) as well as the SEI calculations were based on the actual electrical power consumed by the MW system during the drying process. Therefore, such calculations (indicated by Eqs. (4) and (5)) strongly depended on the conversion efficiency of the delivered electrical power to the MW energy (i.e., on the MW generation efficiency) (Lakshmi et al., 2007; Jang et al., 2011). Such MW generation efficiency was previously reported by Kocbek et al. (2020) for the same MW system at 72% when working at a MW power output of 6 kW (as in this study).

Figs. 6 and 7 illustrate the SEI and energy efficiency as a function of the sludge moisture content for all the evaluated samples. All the sludge samples were dried up to a final moisture content of 0.18 kg of water kg of dry $solids^{-1}$. From looking at Figs. 6 and 7, it can be observed that the lower the initial moisture content of the sludge sample (for instance sample

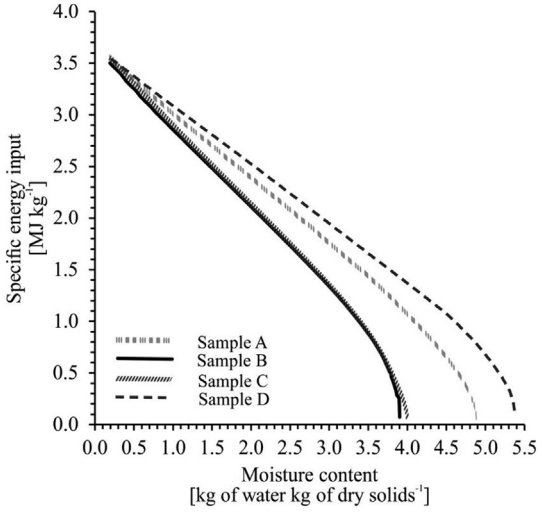

Fig. 6. Specific energy input as a function of moisture content for the evaluated sludge samples.

B vs sample D), the lower the SEI required to reach certain degree of dryness; therefore, the higher the energy efficiency to reach that particular level of moisture content (or DS content). Both figures closely follow the trends previously observed regarding the changes in the sludge moisture content and drying rates as presented in Section 3.2. For instance, at the start of the drying process, an adaptation drying rate period can be observed. In this period, the energy was used for increasing the temperature of the sludge. The energy efficiency values reported in Fig. 7 were calculated following the Eq. (5). Such equation includes in the nominator both the latent heat, and the heat capacity of the water. So, at the early stages of the drying process (when the drying process was started) the sludge sample was mostly being heated without any or little water being evaporated. So, the theoretical energy demand (as expressed in the numerator of Eq. (5)) mostly considered the heat capacity of heating the water, which is relatively small compared to the latent heat of evaporation (since little or no water was evaporated at that time). Therefore, that efficiency term showed in Fig. 7 exhibited low values corresponding to that adaptation drying phase. Given that most of the MW energy was used to increase the temperature of the sludge, only small amounts of water were actually removed. Following the adaptation phase period, there were marginal changes both in the changes of the SEI as a function of the moisture content, as well as

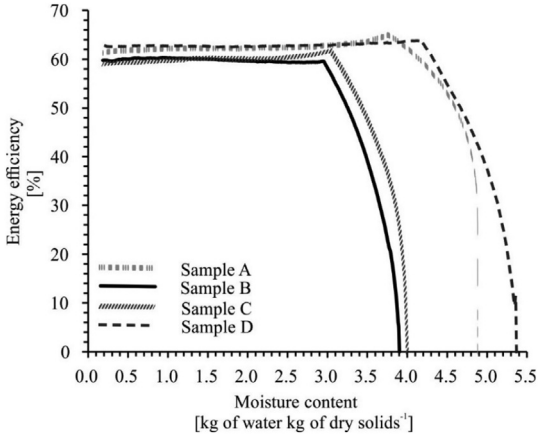

Fig. 7. Energy efficiency as a function of moisture content for the evaluated sludge samples.

in the and energy efficiencies as a function of the moisture content for all the evaluated samples (Figs. 6 and 7). This could be explain considering that the system was removing the surface water of the material at steady-state conditions (i.e., in the constant drying rate period). Looking from an energy performance standpoint, it was not possible to observe the final falling rate drying period in Figs. 6 and 7 as observed in Fig. 5. A similar situation was observed and reported by Kocbek et al. (2020).

The energy performance of the MW system seemed to vary depending on the sludge composition. For instance, when drying the different sludge samples up to a moisture content of 2.5 kg of water kg of dry solids^{-1}, the SEI required for the SS sample (D), as shown in Fig. 6, was 2.2 MJ kg^{-1} (0.6 kWh kg^{-1}) compared to the SEI required for WAS sample B of 1.7 MJ kg^{-1} (0.5 kWh kg^{-1}). These differences become less pronounced as the water is being removed from the sludge samples. For instance, at the end of the drying process the SEIs were similar across the entire range of evaluated samples averaging 3.5 ± 0.07 MJ kg^{-1} (1.0 ± 0.02 kWh kg^{-1}). As described in Section 3.2, that behavior could be related to both the efficiency of the MW absorption, as well as to the conversion of the electromagnetic energy into heat mostly governed by the dielectric properties of the material. These properties strongly depend both on the sludge moisture content, and on the distribution of the water fractions within the material (i.e., the free and bound water content). For instance, sludge samples with a higher amount of free water exhibited a high energy absorption rate within the material; thus, large sludge heating and drying rates inducing a pressure driven flow that is enhanced when considering treatment of high moisture materials (Fig. 5). This could also lead to the extended constant drying rate period associated with the removal of unbound water as observed in Fig. 5. In turns, as explained in Section 3.2, higher sludge drying rate were observed in those sludge sample having a higher proportion of free water than bound water. When particularly focusing on the energy requirement and overall energy efficiency, Figs. 6 and 7, show that the SS sample (D), characterized with the highest initial water content (and also free water content) from all the evaluated samples, required initially the highest SEI to evaporated the initial amounts of water; however, the SEI requirements to completely dry the material up to 0.18 kg of water kg of dry solids^{-1} was similar as for the other evaluated samples. When looking at the energy efficiency (Fig. 7), it was observed that the energy efficiency for the SS (sample D) also reached higher energy efficiency values at higher moisture contents compared to the other evaluated sludge samples. For instance, the SS (sample D) reached energy efficiency values higher than 60% at moisture contents as high as 4.5 kg of water kg of dry solids^{-1} compared to the rest of the evaluated sludge samples that reached that level of energy efficiency somewhere between 3 and 4 kg of water kg of dry solids^{-1}.

The sludge physical-chemical properties exhibited an important role in determining the MW energy absorption performance, which may explain the overall energy efficiency performance and SEI requirements. The MW energy absorption and conversion into heat increased with the amount of free and loosely bound water fraction present in the sludge samples. This had an effect extending the duration of the constant drying period phase, leading to an overall increase in the MW energy efficiency and similar SEI (Fig. 6). Thus, the higher the concentration of free water in the sludge, the more energy-efficient MW drying process (both heating the sludge sample and evaporating the water out of the sludge). The amount of free and loosely bound water molecules was found to be dependent on several physical-chemical properties including the sludge organic content and the concentration of hydrophobic compounds present in the sludge such as the presence of oils and grease. The oil and grease content could also have a positive impact both on the energy needs to increase the temperature of the sludge, as well as on contributing to a more uniform temperature distribution within the bulk material. Similarly, the sludge porosity could positively impact the water flow out of the sludge, improving the MW drying and energy performance. A more detailed discussion pertaining to the effect of sludge physical-chemical properties on MW performance is given in Section 3.2. Therefore, these results indicate that the origin of sludge, as well as the wastewater treatment and stabilization process at which that sludge has been exposed, have a large influence on the physical-

chemical characteristics of sludge and as such on the MW system performance. Examining such properties may contribute to better understanding and optimising the MW sludge drying performance.

4. Conclusions

- Both the origin of the sludge (SS vs WAS), as well as the type of wastewater treatment process and biological stabilization processes at which the sludge was exposed impacted on the physical-chemical characteristics of the sludge including the moisture content, organic content, porosity, presence of hydrophobic compounds, and the water molecule-sludge interactions, among others.
- The MW drying extends the constant rate drying period, thereby accelerating the free water evaporation from the surface of the material which occurs almost independently of the type of sludge that was irradiated.
- The MW energy absorbed by the material on a given time interval is a critical parameter influencing the duration and intensity of the MW drying process; such energy absorption process depends on the dielectric properties of the materials.
- The MW absorption efficiency increased with an increase in the free water content of the sludge; thus, contributing to higher heating rates and increasing the system throughput treatment capacity.
- The MW drying performance depends on the physical-chemical properties of the sludge. Sludge containing a high fraction of free (unbound) water efficiently absorb and convert MW energy into heat
- The sludge unbound water content was higher in the sludge samples showing high concentrations of oil and grease compounds and low organic matter content. These conditions were favoured in septic tanks. Thus, the SS (sample D) absorbed and converted MW energy into heat more efficiently compared to the WAS samples derived from WWTP.

Supplementary data to this article can be found online at https://doi.org/10.1016/j.scitotenv.2022.154142.

CRediT authorship contribution statement

Eva Kocbek: Methodology, Validation, Formal analysis, Investigation, Visualization, Writing – original draft. **Hector A. Garcia:** Supervision, Visualization, Writing – review & editing, Project administration. **Christine M. Hooijmans:** Supervision, Writing – review & editing. **Ivan Mijatović:** Conceptualization, Supervision. **Davor Kržišnik:** Investigation, Visualization, Writing – review & editing. **Miha Humar:** Supervision, Writing – review & editing. **Damir Brdjanovic:** Conceptualization, Writing – review & editing, Supervision, Funding acquisition, Project administration.

Declaration of competing interest

The authors declare that they have no known competing financial interests or personal relationships that could have appeared to influence the work reported in this paper.

Acknowledgement

This research project was developed and funded within the framework of Programmatic cooperation between the Dutch Ministry of Foreign Affairs and IHE Delft (DUPC2) project and is aimed to provide a portable MW-based treatment system for onsite faecal sludge treatment for the humanitarian and development WASH sector. Tehnobiro d.o.o and the Public Scholarship, Development, Disability and Maintenance Fund of the Republic of Slovenia provided a PhD fellowship for one of the researchers involved in this study. The authors would like to thank the staff of tehnobiro d.o.o., (Maribor, Slovenia), Central wastewater treatment plant Ptuj (Ptuj, Slovenia) and the Chemical Laboratory of the Public Utility Company Ptuj (Ptuj, Slovenia) for their technical and valuable support during this study.

References

Andrade, R.D., Lemus, R., CEJV, Perez, 2011. Models of Sorption Isotherms for Food: Uses and Limitations. 18, pp. 325–334 (3).
Antunes, E., Jacob, M.V., Brodie, G., Schneider, P.A., 2018. Microwave pyrolysis of sewage biosolids: dielectric properties, microwave susceptor role and its impact on biochar properties. J. Anal. Appl. Pyrolysis 129, 93–100.
Beneroso, D., Monti, T., Kostas, E.T., Robinson, J., 2017. Microwave pyrolysis of biomass for bio-oil production: scalable processing concepts. Chem. Eng. J. 316, 481–498.
Bennamoun, L., Chen, Z., Afzal, M.T., 2016. Microwave drying of wastewater sludge: experimental and modeling study. Dry. Technol. 34 (2), 235–243.
Berk, Z., 2018. Food Process Engineering and Technology. Academic Press.
Bilecka, I., Niederberger, M., 2010. Microwave chemistry for inorganic nanomaterials synthesis. Nanoscale 2 (8), 1358–1374.
Bougayr, E.H., Lakhal, E.K., Idlimam, A., Lamharrar, A., Kouhila, M., Berroug, F., 2018. Experimental study of hygroscopic equilibrium and thermodynamic properties of sewage sludge. Appl. Therm. Eng. 143, 521–531.
Candanedo, L., Derome, D., 2005. Numerical simulation of water absorption in softwood. Paper Presented at the Proceedings of the 9th International IBPSA Conference, August.
Chen, Z., Afzal, M.T., Salema, A.A., 2014. Microwave drying of wastewater sewage sludge. J. Clean Energy Technol. 2 (3), 282–286.
Clark, D.E., Folz, D.C., West, J.K., 2000. Processing materials with microwave energy. Mater. Sci. Eng. A 287 (2), 153–158.
Collard, M., Teychené, B., Lemée, L., 2017. Comparison of three different wastewater sludge and their respective drying processes: solar, thermal and reed beds – impact on organic matter characteristics. J. Environ. Manag. 203, 760–767.
Cui, Y., Ravnik, J., Steinmann, P., Hriberšek, M., 2019. Settling characteristics of nonspherical porous sludge flocs with nonhomogeneous mass distribution. Water Res. 158, 159–170.
Dealler, S.F., Rotowa, N.A.L., Richard, W., 1992. Ionized molecules reduce penetration of microwaves into food. Int. J. Food Sci. Technol. 27 (2), 153–157.
Dominguez, A., Menéndez, J., Inguanzo, M.P., 2004. Sewage sludge drying using microwave energy and characterization by IRTF. Afinidad 61 (512), 280–285.
Doran, P.M., 2013. Chapter 11 - unit operations. In: Doran, P.M. (Ed.), Bioprocess Engineering Principles, Second edition Academic Press, London, pp. 445–595.
Du, G., Wang, S., Cai, ZJDt, 2005. Microwave Drying of Wood Strands. 23, pp. 2421–2436 (12).
Đurđević, D., Trstenjak, M., Hulenić, I., 2020. Sewage sludge thermal treatment technology selection by utilizing the analytical hierarchy process. Water 12 (5), 1255.
Earle, R., Earle, M., 2004. Unit Operations in Food Processing, Web Edition. The New Zealand.
Fassinou, W.F., 2012. Higher heating value (HHV) of vegetable oils, fats and biodiesels evaluation based on their pure fatty acids' HHV. Energy 45 (1), 798–805.
Federation and Association, W.E. Federation, American Public Health Association, 2005. Standard Methods for the Examination of Water and Wastewater. American Public Health Association (APHA), Washington, DC, USA.
Feng, G., Tan, W., Zhong, N., Liu, L., 2014. Effects of thermal treatment on physical and expression dewatering characteristics of municipal sludge. Chem. Eng. J. 247, 223–230.
Feng, G., Bai, T., Ma, H., Hu, Z., Guo, Y., Tan, W., 2019. Establishment of the permeability model for soft solid sludge conditioned with flocculants. ACS Omega 4 (20), 18574–18581.
Flaga, A., 2005. Sludge drying. Paper Presented at the Proceedings of Polish-Swedish Seminars, Integration and Optimization of Urban Sanitation Systems. Cracow March.
Freire, F., Freire, F.B., Pires, E., Freire, JJEt, 2007. Moisture Adsorption and Desorption Behavior of Sludge Powder. 28, pp. 1195–1203 (11).
Friedl, A., Padouvas, E., Rotter, H., Varmuza, K., 2005. Prediction of heating values of biomass fuel from elemental composition. Anal. Chim. Acta 544 (1), 191–198.
Fu, B., Chen, M., Song, J., 2017. Investigation on the microwave drying kinetics and pumping phenomenon of lignite spheres. Appl. Therm. Eng. 124, 371–380.
Gomes, L.A., Gabriel, N., Gando-Ferreira, L.M., Góis, J.C., Quina, M.J., 2019. Analysis of potentially toxic metal constraints to apply sewage sludge in Portuguese agricultural soils. Environ. Sci. Pollut. Res. 26 (25), 26000–26014.
Guo, J., Zheng, L., Li, Z., 2021. Microwave drying behavior, energy consumption, and mathematical modeling of sewage sludge in a novel pilot-scale microwave drying system. Sci. Total Environ. 777, 146109.
Gupta, M., Leong, E.W.W., 2007. Microwaves and Metals. John Wiley & Sons.
Hailwood, A., Horrobin, SJTotFS, 1946. Absorption of Water by Polymers: Analysis in Terms of a Simple Model. 42, pp. B084–B092.
Haque, K.E., 1999. Microwave energy for mineral treatment processes—a brief review. Int. J. Miner. Process. 57 (1), 1–24.
Hong, S.M., Park, J.K., Lee, Y., 2004. Mechanisms of microwave irradiation involved in the destruction of fecal coliforms from biosolids. Water Res. 38 (6), 1615–1625.
Hong, S.M., Park, J.K., Teeradej, N., Lee, Y., Cho, Y., Park, C., 2006. Pretreatment of sludge with microwaves for pathogen destruction and improved anaerobic digestion performance. Water Environ. Res. 78 (1), 76–83.
Jafari, H., Kalantari, D., Azadbakht, M., 2018. Energy consumption and qualitative evaluation of a continuous band microwave dryer for rice paddy drying. Energy 142, 647–654.
Jang, S.-R., Ryoo, H.-J., Ahn, S.-H., Kim, J., Rim, G.H., 2011. Development and optimization of high-voltage power supply system for industrial magnetron. Trans. Ind. Electron. 59 (3), 1453–1461.
Jones, S.B., Or, D., 2003. Modeled effects on permittivity measurements of water content in high surface area porous media. Phys. B Condens. Matter 338 (1), 284–290.
Kamran, K., Gao, N., 2020. Thermochemical conversion of sewage sludge: a critical review. Prog. Energy Combust. Sci. 79.
Kehrein, P., van Loosdrecht, M., Osseweijer, P., Garfí, M., Dewulf, J., Posada, J., 2020. A critical review of resource recovery from municipal wastewater treatment plants–market

supply potentials, technologies and bottlenecks. Environ. Sci. Water Res. Technol. 6 (4), 877–910.
Kelessidis, A., Stasinakis, A.S., 2012. Comparative study of the methods used for treatment and final disposal of sewage sludge in European countries. Waste Manag. 32 (6), 1186–1195.
Khanlari, A., Sözen, A., Afshari, F., Şirin, C., Tuncer, A.D., Gungor, A., 2020. Drying municipal sewage sludge with v-groove triple-pass and quadruple-pass solar air heaters along with testing of a solar absorber drying chamber. Sci. Total Environ. 709, 136198.
Kocbek, E., Garcia, H.A., Hooijmans, C.M., Mijatović, I., Lah, B., Brdjanovic, D., 2020. Microwave treatment of municipal sewage sludge: evaluation of the drying performance and energy demand of a pilot-scale microwave drying system. Sci. Total Environ. 742, 140541.
Kocbek, E., Garcia, H.A., Hooijmans, C.M., Mijatović, I., Al-Addous, M., Dalala, Z., Brdjanovic, D.J.E.S., Research P, 2021. Novel Semi-decentralised Mobile System for the Sanitization and Dehydration of Septic Sludge: A Pilot-scale Evaluation in the Jordan Valley, pp. 1–21.
Kouchakzadeh, A., Shafeei, S., 2010. Modeling of microwave-convective drying of pistachios. Energy Convers. Manag. 51 (10), 2012–2015.
Kroiss, H., Zessner, M., 2007. Ecological and Economical Relevance of Sludge Treatment and Disposal Options.
Kumar, C., Joardder, M., Farrell, T.W., Karim, M., 2016. Multiphase porous media model for intermittent microwave convective drying (IMCD) of food. Int. J. Therm. Sci. 104, 304–314.
Lakshmi, S., Chakkaravarthi, A., Subramanian, R., Singh, V., 2007. Energy consumption in microwave cooking of rice and its comparison with other domestic appliances. J. Food Eng. 78 (2), 715–722.
Lam, C.M., Hsu, S.-C., Alvarado, V., Li, W.M., 2020. Integrated life-cycle data envelopment analysis for techno-environmental performance evaluation on sludge-to-energy systems. Appl. Energy 266, 114867.
LeBlanc, R.J., Matthews, P., Richard, R.P., 2009. Global Atlas of Excreta, Wastewater Sludge, and Biosolids Management: Moving Forward the Sustainable and Welcome Uses of a Global Resource. Un-habitat.
Ledakowicz, S., Stolarek, P., Malinowski, A., Lepez, O., 2019. Thermochemical treatment of sewage sludge by integration of drying and pyrolysis/autogasification. Renew. Sust. Energ. Rev. 104, 319–327.
Léonard, A., Vandevenne, P., Salmon, T., Marchot, P., Crine, M., 2004. Wastewater sludge convective drying: influence of sludge origin. Environ. Technol. 25 (9), 1051–1057.
Li, J., Fraikin, L., Salmon, T., Plougonven, E., Toye, D., Léonard, A., 2016. Convective drying behavior of sawdust-sludge mixtures in a fixed bed. Dry. Technol. 34 (4), 395–402.
Lyng, J.G., Arimi, J.M., Scully, M., Marra, F., 2014. The influence of compositional changes in reconstituted potato flakes on thermal and dielectric properties and temperatures following microwave heating. J. Food Eng. 124, 133–142.
Ma, R., Yuan, N., Sun, S., Zhang, P., Fang, L., Zhang, X., Zhao, X., 2017. Preliminary investigation of the microwave pyrolysis mechanism of sludge based on high frequency structure simulator simulation of the electromagnetic field distribution. Bioresour. Technol. 234, 370–379.
Macías-García, A., Díaz-Díez, M.A., Alfaro-Domínguez, M., Carrasco-Amador, J.P., 2020. Influence of chemical composition, porosity and fractal dimension on the electrical conductivity of carbon blacks. Heliyon 6 (6), e04024.
Maskan, M., 2000. Microwave/air and microwave finish drying of banana. J. Food Eng. 44 (2), 71–78.
Maskan, MJJofe, 2001. Drying, Shrinkage and Rehydration Characteristics of Kiwifruits During Hot Air and Microwave Drying. 48, pp. 177–182 (2).
Mawioo, P.M., Hooijmans, C.M., Garcia, H.A., Brdjanovic, D., 2016a. Microwave treatment of faecal sludge from intensively used toilets in the slums of Nairobi, Kenya. J. Environ. Manag. 184, 575–584.
Mawioo, P.M., Rweyemamu, A., Garcia, H.A., Hooijmans, C.M., Brdjanovic, D., 2016b. Evaluation of a microwave based reactor for the treatment of blackwater sludge. Sci. Total Environ. 548, 72–81.
Mawioo, P.M., Garcia, H.A., Hooijmans, C.M., Velkushanova, K., Simonič, M., Mijatović, I., Brdjanovic, D., 2017. A pilot-scale microwave technology for sludge sanitization and drying. Sci. Total Environ. 601, 1437–1448.
Mishra, R.R., Sharma, A.K., 2016. Microwave–material interaction phenomena: heating mechanisms, challenges and opportunities in material processing. Compos. A: Appl. Sci. Manuf. 81, 78–97.
Mujumdar, A.S., 2014. Handbook of Industrial Drying. 4th ed. CRC Press.
Mujumdar, A.S., Devahastin, S., 2000. Fundamental principles of drying. Mujumdar's Practical Guide to Industrial Drying. Exergex Corporation, Canada.
Ni, H., Datta, A., Torrance, K., 1999. Moisture transport in intensive microwave heating of biomaterials: a multiphase porous media model. Int. J. Heat Mass Transf. 42 (8), 1501–1512.
Ohm, T.-I., Chae, J.-S., Kim, J.-E., Kim, H.-k., Moon, S.-H., 2009. A study on the dewatering of industrial waste sludge by fry-drying technology. J. Hazard. Mater. 168 (1), 445–450.
Peal, A., Evans, B., Blackett, I., Hawkins, P., Heymans, C., 2014. Fecal sludge management: a comparative analysis of 12 cities. J. Water Sanit. Hyg. Dev. 4 (4), 563–575.
Peleg, M., 2020. Models of sigmoid equilibrium moisture sorption isotherms with and without the monolayer hypothesis. Food Eng. Rev. 12 (1), 1–13.
Penfield, M.P., Campbell, A.M., 1990. Chapter 6 - introduction to food science. In: Penfield, M.P., Campbell, A.M. (Eds.), Experimental Food Science, Third edition Academic Press, San Diego, pp. 97–129.
Pickles, C., Gao, F., Kelebek, S., 2014. Microwave drying of a low-rank sub-bituminous coal. Miner. Eng. 62, 31–42.
Pino-Jelcic, S.A., Hong, S.M., Park, J.K., 2006. Enhanced anaerobic biodegradability and inactivation of fecal coliforms and Salmonella spp. in wastewater sludge by using microwaves. Water Environ. Res. 78 (2), 209–216.
Pitchai, K., Birla, S.L., Subbiah, J., Jones, D., Thippareddi, H., 2012. Coupled electromagnetic and heat transfer model for microwave heating in domestic ovens. J. Food Eng. 112 (1), 100–111.
Poyet, S., Charles, S., 2009. Temperature dependence of the sorption isotherms of cement-based materials: heat of sorption and Clausius-Clapeyron formula. Cem. Concr. Res. 39 (11), 1060–1067.
Radomski, J.L., Krischer, KNJJotNCI, Krischer, C., 1978. Histologic and Histochemical Preneoplastic Changes in the Bladder Mucosae of Dogs Given 2-Naphthylamine. 60, pp. 327–333 (2).
Schulz, R., Ray, N., Zech, S., Rupp, A., Knabner, P., 2019. Beyond Kozeny–Carman: predicting the permeability in porous media. Transp. Porous Media 130 (2), 487–512.
Soltysiak, M., Erle, U., Celuch, M., 2008. Load curve estimation for microwave ovens: experiments and electromagnetic modelling. Paper Presented at the MIKON 2008–17th International Conference on Microwaves, Radar and Wireless Communications.
Sousa, K.Ad., Resende, O., Carvalho, Bd.S., 2016. Determination of desorption isotherms, latent heat and isosteric heat of Pequi diaspore. Rev. Bras. Eng. Agríc. Ambiental 20 (5), 493–498.
Stuerga, D., 2006. Microwave-material Interactions and Dielectric Properties, Key Ingredients for Mastery of Chemical Microwave Processes. 2. WILEY-VCH Verlag GmbH & Co. KGaA.
Tao, T., Peng, X., Lee, D., 2005. Structure of crack in thermally dried sludge cake. Dry. Technol. 23 (7), 1555–1568.
Vaxelaire, JJJoCT, 2001. Moisture sorption characteristics of waste activated sludge. Biotechnol. Int. Res. Process E Technol C 76 (4), 377–382.
Vesilind, P.A., 1994. The role of water in sludge dewatering. Water Environ. Res. 66 (1), 4–11.
Wiśniowska, E., Grobelak, A., Kokot, P., Kacprzak, M., 2019. 10 - sludge legislation-comparison between different countries. In: Prasad, M.N.V., de Campos Favas, P.J., Vithanage, M., Mohan, S.V. (Eds.), Industrial and Municipal Sludge. Butterworth-Heinemann, pp. 201–224.
Yiotis, A.G., Tsimpanogiannis, I.N., Stubos, A.K., 2010. Fractal characteristics and scaling of the drying front in porous media: a pore network study. Dry. Technol. 28 (8), 981–990.
Zhang, S., Zhou, L., Ling, B., Wang, S., 2016. Dielectric properties of peanut kernels associated with microwave and radio frequency drying. Biosyst. Eng. 145, 108–117.
Zhang, J., Li, M., Cheng, J., Wang, J., Ding, Z., Yuan, X., Zhou, S., Liu, X., 2019a. Effects of moisture, temperature, and salt content on the dielectric properties of pecan kernels during microwave and radio frequency drying processes. Foods (Basel, Switzerland) 8 (9), 385.
Zhang, X., Kang, H., Zhang, Q., Hao, X., Han, X., Zhang, W., Jiao, T., 2019b. The porous structure effects of skeleton builders in sustainable sludge dewatering process. J. Environ. Manag. 230, 14–20.